network on hydrophobic surfaces will be favored when the surface is uniform and smooth. The importance of the surface hydrophobicity in bringing about long-range attraction has been pointed out by previous workers.[8,10] It is clear that our monolayer modified mica which is sufficiently large, molecularly smooth, and strongly hydrophobic is the prerequisite for the observed long-range attraction. Numerous physiological anomalies at the biological surface were referred to the structuring of the vicinal water.[5,28] We consider that the observed attractive force has significant bearing on biological functions at cell surfaces.

Acknowledgment. We appreciate Dr. Shinji Kato for providing polymerized amphiphile **1**. We thank referees for their valuable comments.

Monte Carlo Simulations for the Interactions of Metal Complexes with the Silicate Sheets of a Clay: Comparison of Binding States between Tris(1,10-phenanthroline)metal(II) and Tris(2,2′-bipyridyl)metal(II) Chelates

Hisako Sato,[†] Akihiko Yamagishi,*[,‡] and Shigeki Kato[§]

Contribution from the Device Development Center, Hitachi Ltd., Imai, Ome-shi, Tokyo 198, Japan, Department of Polymer Science, Hokkaido University, Sapporo 060, Japan, and Department of Chemistry, Faculty of Science, Kyoto University, Sakyo-ku, Kyoto 606, Japan.
Received April 13, 1992. Revised Manuscript Received September 23, 1992

Abstract: Monte Carlo simulations are used to compare the binding states of tris(1,10-phenanthroline)metal(II) ($[M(phen)_3]^{2+}$) and tris(2,2′-bipyridyl)metal(II) ($[M(bpy)_3]^{2+}$) bound to a clay. A pair of $[M(phen)_3]^{2+}$ or $[M(bpy)_3]^{2+}$ complexes is placed on the model surface of a silicate sheet. The surface is composed of linked $[SiO_4]^{4-}$ and $[AlO_4]^{5-}$ tetrahedra. The binding energy is obtained as the sum of the interaction energies of the metal complexes with the sheet and the intermolecular energy between the metal complexes. The stable binding state is examined in terms of the free energy at 300 K as a function of the intermolecular distance, r_{M-M}. For $[M(phen)_3]^{2+}$, a racemic pair has the minimum free energy at r_{M-M} = 9.2 Å, and an enantiomeric pair has the minimum free energy at r_{M-M} = 13.4 Å. The mean binding energy (E) for the racemic pair is 1.5 kJ/mol lower than that for the enantiomeric pair. The results indicate that the racemic mixture forms a more compact and stable pair than does the pure enantiomer. For $[M(bpy)_3]^{2+}$, racemic and enantiomeric pairs have the minimum binding free energy at nearly the same values of r_{M-M}: r_{M-M} = 9.3 Å for a racemic pair and 9.5 Å for an enantiomeric pair. E is 25.3 kJ/mol lower for the racemic pair than for the enantiomeric pair. Thus a pair of the metal complexes form a dimer with similar compactness irrespective of the chirality of the complexes. These results are compared with experimental observations of the chirality effects on the adsorption behaviors of these metal complexes by a clay.

Introduction

Clay minerals are phyllosilicates with layer structures. For the 2:1 class of clays, a layer is composed of an octahedral sheet sandwiched by two tetrahedral sheets.[1] The surface of a tetrahedral sheet is characterized by a two-dimensional network structure, as confirmed by electron diffraction analyses and AFM observations.[2,3]

Recently, the remarkable effect of chirality on the amount of adsorption of a metal complex by a clay has been reported.[4-6] For example, when $[M(phen)_3]^{2+}$ (phen = 1,10-phenanthroline) and $[M(bpy)_3]^{2+}$ (bpy = 2,2′-bipyridyl) are adsorbed, the maximum amount of adsorption is different between a racemic mixture and a pure enantiomer. The racemic mixture of $[M(phen)_3]^{2+}$ (M = Fe and Ru) is adsorbed to about a 2-fold excess of the cation-exchange capacity (CEC), while the enantiomer is adsorbed at levels within the CEC.[7] In the case of $[M(bpy)_3]^{2+}$ (M = Ru), a counter anion affects the adsorption behaviors drastically. At low ionic strength, the racemic mixture is adsorbed at levels within the CEC, while the enantiomer of the same chelate is adsorbed in 1.5–2.5-fold excess of the CEC. At high ionic strength, both the racemic mixture and enantiomer of $[M(bpy)_3]^{2+}$ are adsorbed in excess of the CEC.[8]

A clay is a unique material in the sense that such an enormous difference in the adsorption amount is not observed for other ion exchangers, such as ion-exchange resins and zirconium phosphate.[4] The above results are considered to be an indication that the bound metal complexes interact with their neighbors in a stereoselective way, leading to the difference in the packing structures between a racemic mixture and a pure enantiomer. It is also suspected on the basis of a simple molecular model that the geometrical matching between the molecular size of a metal complex and the network structure of a silicate sheet is essential to achieving these stereoselective interactions.[4] These properties have opened the way to utilizing a clay–metal complex adduct as an adsorbent in optical resolution and asymmetric syntheses.[5,6]

Extensive work has been done to validate the above postulate. No decisive experimental evidence, however, has so far been presented.[9] In this work, the adsorption of metal complexes by

[†] Hitachi Ltd.
[‡] Hokkaido University.
[§] Kyoto University.

(1) Brindley, G. W.; Brown, G. *Crystal Structures of Clay Minerals and Their X-Ray Identification*; Mineralogical Society: London, 1980; Chapter 1.
(2) Cowley, J. M.; Gaswami, A. *Acta Crystallogr.* **1961**, *14*, 1071.
(3) Hartman, H.; Spasito, G.; Yang, A.; Mame, S.; Gorld, S. A. C.; Haneme, P. K. *Clays Clay Miner.* **1990**, *38*, 337.
(4) (a) Yamagishi, A. *J. Am. Chem. Soc.* **1981**, *103*, 4640. (b) Yamagishi, A. *J. Coord. Chem.* **1987**, *16*, 131.
(5) Nakamura, Y.; Yamagishi, A.; Matsumoto, S.; Tohkubo, K.; Ohtsu, Y.; Yamaguchi, M. *J. Chromatogr.* **1989**, *482*, 165.
(6) Hikita, T.; Tamaru, K.; Iwamoto, T.; Yamagishi, A. *Inorg. Chem.* **1989**, *28*, 2221.
(7) Yamagishi, A. *J. Phys. Chem.* **1982**, *86*, 2474.
(8) (a) Villemure, G. *Clays Clay Miner.* **1990**, *38*, 622. (b) Villemure, G. *Clays Clay Miner.* **1991**, *39*, 580.

0002-7863/92/1514-10933$03.00/0

a clay is studied theoretically. We use a model wherein a racemic or an enantiomeric pair of metal complexes is bound by a sheet of linked $[SiO_4]^{4-}$ and $[AlO_4]^{5-}$ tetrahedra in water medium. We consider an isolated pair of bound metal complexes which may be formed at low loading. Monte Carlo methodology is applied to obtain the distributions of configurations at thermal equilibrium. The free energy of the system is obtained as a function of the intermolecular distance between the metal complexes. The stereochemical effects on the intermolecular interactions are investigated in detail. The results are compared between the racemic and enantiomeric pairs of the $[M(phen)_3]^{2+}$ and $[M(bpy)_3]^{2+}$ systems.

Previously, several theoretical works have been reported on the chiral discriminations for homo- and heterochiral molecular pairs such as tris(butadienyl) complexes, tripodal-shaped molecules forming a Langmuir monolayer and tetrahedral molecules.[10,11] The present work is an extension of these theoretical works to chiral molecules adsorbed on a solid surface, using a Monte Carlo simulation. The same method has been applied recently to obtain the cohesive energies of clay layers.[12]

Methods

(1) Binding Energy. The total binding energy of metal complexes on silicate sheets, E, is equal to the sum of the interaction energies of the metal complexes with the silicate sheet (E_{M1-C} and E_{M2-C}) and the intermolecular interaction between the metal complexes (E_{M-M}), as below:

$$E = E_{M1-C} + E_{M2-C} + E_{M-M} \quad (1)$$

In the case of a single metal complex, E contains only the E_{M1-C} term. Each term in the above equation is expressed as the sum of the electrostatic energy (E_{es}) and the short-range interaction energy (E_{vw}):

$$E = E_{es} + E_{vw} \quad (2)$$

These energies are given by the atom–atom pair potentials between two atoms:

$$E_{es} = \sum_i \sum_j e_i^* e_j^* / r_{ij} \quad (3)$$

where e_i and e_j are the effective charges on the ith and jth atoms, respectively, and r_{ij} denotes the interatomic distance.

The short-range interaction energy E_{vw} between the ith and jth atoms is expressed as the Lennard-Jones potential,[13]

$$E_{vw} = \sum_i \sum_j 4U_{0ij}[(\sigma_{ij}/r_{ij})^{12} - (\sigma_{ij}/r_{ij})^6] \quad (4)$$

in which the energy and length parameters are approximated by

$$U_{0ij} = (U_i U_j)^{0.5} \quad (5)$$

$$\sigma_{ij} = 0.5(\sigma_i + \sigma_j) \quad (6)$$

with the values of U_i and σ_i intrinsic to the ith atom. The short-range interactions are calculated for a hydrogen atom, a carbon atom, a nitrogen atom, an oxygen atom, and a chloride ion.[14,15]

(2) Effective Charges. Two quantities for the effective charges of atoms were examined: the Mulliken atomic charge ($e(MK)_i^*$)[16] and the electrostatic effective charge ($e(ES)_i^*$), which is derived directly from the electrostatic potential.[17] Mulliken atomic charges were used for the effective charges of metal complexes, and electrostatic effective charges were used for the effective charges of a silicate sheet.

In order to obtain the $e(MK)_i^*$ values of a metal complex, ab initio molecular orbital calculations were performed, neglecting the electronic interactions between the ligands and a central metal ion, M(II) or M(III) (HONDO7, QCPE544).[18] The structures of $[M(phen)_3]^{2+}$ (and $[M(phen)_3]^{3+}$) and $[M(en)_3]^{3+}$ (en = ethylenediamine) are assumed to be the same as those of $[Fe(phen)_3]^{2+}$ and $[Co(en)_3]^{3+}$, respectively.[19a,b] For $[M(bpy)_3]^{2+}$, the metal-to-ligand distance is assumed to be the same as that of $[M(phen)_3]^{2+}$. No optimization of the structure of a metal complex was carried out. The restricted Hartree–Fock (RHF) wave function with the STO-3G minimal basis set was employed.

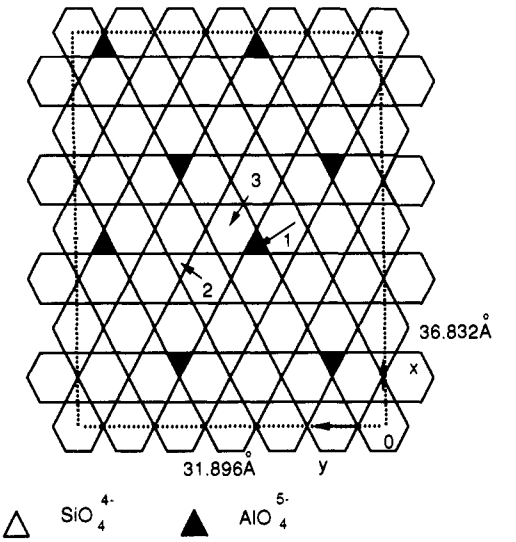

Figure 1. The model silicate sheet, corresponding to a unit cell used in the Metropolis method. The empty and filled triangles denote $[SiO_4]^{4-}$ and $[AlO_4]^{5-}$ tetrahedra, respectively. The arrows numbered 1, 2, and 3 denote the initial positions of chelates for simulation calculations (see text).

In order to determine the $e(ES)_i^*$ values of a silicate sheet, the electrostatic energy due to the electron density at a position r, $\rho(r)$, and the nuclear charge, Z_i, was calculated.

$$V_{es}(r) = \int dr' \rho(r)/|r - r'| + \sum_i Z_i/|r - r'| \quad (7)$$

Here $\rho(r)$ is determined by ab initio molecular orbital methods for a small cluster, and $e(ES)_i^*$ is determined by fitting the potential $V_{es}(r)$ to the function

$$V_{es}(r) = \sum_i e(ES)_i^*/|r_i - r| \quad (8)$$

The electrostatic potential was calculated at about 600 points for each cluster.

(3) Geometry of a Cluster. The structure of a $[SiO_4]^{4-}$ moiety is assumed to have the normal tetrahedral form. The Si–O distance is taken from the experimental value for α-quartz, 1.628 Å.[20] The Al–O distance is assumed to be the same as the Si–O distance, although the former is reported to be about 0.05 Å longer than the latter.[20] Since we used the cluster model to simulate the clay surface, hydrogen atoms were attached to the terminal oxygen atoms to represent the sp^3 hybridization of the oxygen atoms, with the OH distance of 0.958 Å taken from the reported value for a water molecule.[20]

(4) Model Clusters for the Tetrahedral Sheet of a Clay. For a model of the tetrahedral sheet of a clay, we used a two-dimensional sheet composed of linked $[SiO_4]^{4-}$ tetrahedra. Some of the $[SiO_4]^{4-}$ tetrahedra were replaced with $[AlO_4]^{5-}$ tetrahedra, as shown in Figure 1. The cluster in the figure corresponds to the tetrahedral sheet of a 2:1 smectite clay in which isomorphous substitutions take place in the tetrahedral sheets. The contribution of an octahedral sheet to the binding energy was taken into account by adding an OH group at the center of a ditrigonal cavity. The direction of the OH bond is perpendicular to the surface. The horizontal position of the O atom is the same as that of the apical O atom in $[SiO_4]^{4-}$. The OH distance was taken to be 0.958 Å.[20]

(5) Monte Carlo Simulations for a Clay–Metal Complex System. The simulations of a bound state are based on Monte Carlo technique using

(9) Taniguchi, M.; Yamagishi, A.; Iwamoto, T. *Inorg. Chem.* **1991**, *30*, 2462.
(10) Kuroda, R.; Mason, S. F.; Rodger, C. D.; Seal, R. H. *Mol. Phys.* **1981**, *42*, 33.
(11) (a) Andelman, D. *J. Am. Chem. Soc.* **1989**, *111*, 6536. (b) Salem, L.; Chapuisat, X.; Segal, G.; Hiberty, P. C.; Minot, C.; Leforestier, C.; Sautet, P. *J. Am. Chem. Soc.* **1987**, *109*, 2887.
(12) Deiville, A.; Laszlo, P. *New J. Chem.* **1989**, *13*, 481.
(13) Burkert, U.; Alinger, N. L. *Molecular Mechanics*; American Chemical Society: Washington, DC, 1982; Chapter 3.
(14) Vega, L.; Breton, J. *J. Chem. Phys.* **1986**, *84*, 5171.
(15) Brooks, B. R.; Bruccoleri, R. E.; Olafson, B. D.; States, D. J.; Swaminathan, S.; Karplus, M. *J. Comput. Chem.* **1983**, *4*, 187.
(16) Mulliken, R. S. *J. Chem. Phys.* **1955**, *23*, 1841.
(17) Kato, S.; Amadatsu, Y. *J. Chem. Phys.* **1990**, *92*, 7241.
(18) HONDO7: program registered in QCPE 544.
(19) (a) Zalkin, A.; Templeton, D. H.; Ueki, T. *Inorg. Chem.* **1973**, *12*, 1641. (b) Witiak, D.; Clardy, J. C.; Martin, D. S., Jr. *Acta Crystallogr.* **1971**, *28B*, 2694.
(20) Gibbs, G. V. *Am. Mineral.* **1982**, *67*, 421.

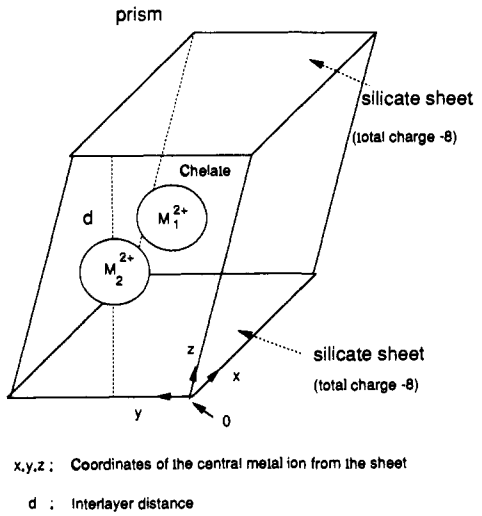

Figure 2. The prism used for the Monte Carlo simulations. This figure shows the binding of a complex ion with a silicate sheet.

a Metropolis algorithm.[21] The Monte Carlo box is a rectangular prism, as shown in Figure 2. The lower surface of the prism is the same as that shown in Figure 1. The upper surface is made by turning the lower surface upside down. The x and y axes were chosen as indicated in the figure, and they coincide with the a and b axes of the unit lattice of a 2:1 clay layer, respectively. The z axis is normal to the sheet surface. The origin of the coordinate is taken at the lower-right edge of the lower sheet. Either a single metal complex or a pair of metal complexes were placed inside the prism. The periodic boundary conditions were applied in both the x and y directions. The orientation of a metal complex is described in terms of Euler angles, where the 3-fold symmetry (C_3) and 2-fold symmetry (C_2) axes coincide with the z and x axes at $\theta = 0$, $\phi = 0$, and $\psi = 0$, respectively (Figure 3). The spatial position and orientation of the metal complex were given random displacements.

The net charge of the unit cell is not 0 when one or two dipositive metal complexes are placed inside the prism. Therefore it is not appropriate to calculate the contribution of the electrostatic energy outside the cell by the Ewald sum method.[21] Instead we apply the method of truncating the electrostatic interaction at the proper distance.[22] For that purpose, the electrostatic energy was modified with the following tapering function:

$$\xi(x) = \begin{cases} 1 & \text{for } x < 0 \\ 1 - x^3[10 - x(15 - 6x)] & \text{for } 0 < x < 1 \\ 0 & \text{for } x > 1 \end{cases} \qquad (9)$$

$$x = (R_{c,m} - R_T)/(R_c - R_T)$$

where $R_{c,m}$ denotes the distance between the central metal of a chelate and an atom in a sheet. The cutoff distance, R_c, was taken to be half of the prism length, and $R_T = 0.9R_c$. The short-range interaction energy was calculated within the cutoff distance R_c. The electrostatic energy was obtained by multiplying eq 1 with eq 9.

Equilibration runs of 10 000 moves were performed prior to all production runs, which comprised 100 000 moves. The individual displacement parameters were adjusted so that the acceptance ratio was about 50%. The temperature of the system was kept constant at $T = 300$ K, and the stability of the binding structure was analyzed in terms of the free energy of the system at that temperature. When the system took a value of i along one of the coordinates, the free energy at i, $\Delta F(i)$, was calculated according to the potential of mean force equation,[17]

$$\Delta F(i) = -kT \ln N(i) \qquad (10)$$

in which $N(i)$ is the number of configurations when the system takes a value of i. $\Delta F(i)$ is taken to be 0 at the minimum value.

(6) Effect of Water Medium. Water is regarded as a dielectric continuum,[23] and eq 3 is replaced with the equation

$$E_{es} = \sum_i \sum_j e_i^* e_j^* / \epsilon r_{ij} \qquad (11)$$

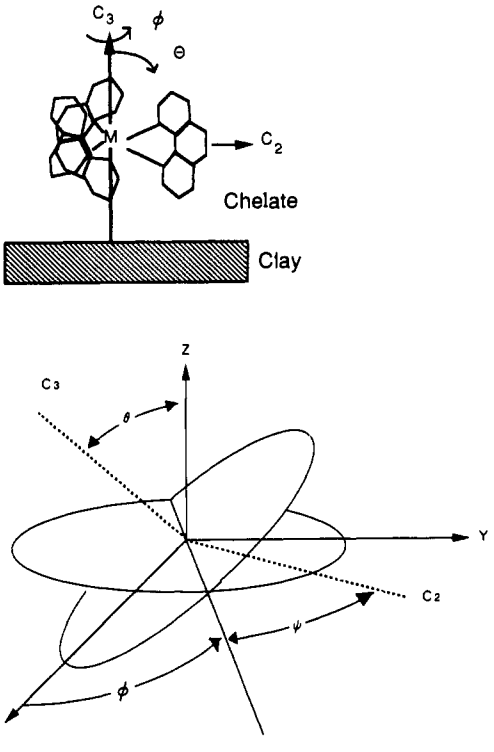

Figure 3. The Euler angles describing the orientation of a metal complex. C_3 and C_2 denote the 3-fold and 2-fold symmetry axes of a metal complex, respectively.

in which the dielectric constant, ϵ, is expressed as a function of the distance r between two charged particles:

$$\epsilon = 39.0\{\tanh [0.8(r - 11)] + 1.05\} \qquad (12)$$

According to eq 12, the dielectric constant varies from 1 at $r = 0$ Å to 80 at $r > 20$ Å.[23]

Results

(1) Binding of a Single $[M(phen)_3]^{2+}$ Molecule on a Silicate Sheet. The binding state of a $[M(phen)_3]^{2+}$ molecule was examined. A Λ isomer is placed inside the prism in Figure 2 at the interlayer distance of 20 Å. It corresponds to a clay partially swelled in water medium. The simulation is started from three initial positions. The first starting position locates the central metal ion in the metal complex 6 Å above the aluminum atom denoted by arrow 1 in Figure 1. This position is chosen because the previous preliminary calculation shows that the metal complex is most stable above the aluminum atom.[24] The second starting position is 6 Å above the silicon atom denoted by arrow 2, and the last is 6 Å above the center of the ditrigonal cavity denoted by arrow 3. The thermal distributions of the configurations are obtained by performing Monte Carlo simulations. The results are given by the contour map of the free energy on the x,y plane shown in Figure 4. In accord with the previous calculation, there exists a deep potential minimum above the aluminum atom. In addition to this, other potential minima exist above the silicon atoms. The metal complex is unstable when the central metal ion is located above the ditrigonal cavity.

Figure 5 shows the binding state of the chelate at the minimum binding energy, in which the central metal ion is located above the aluminum atom in a sheet. The 3-fold symmetry (C_3) axis is perpendicular to the surface. The hydrogen atom at the bottom of each ligand is located near the center of a ditrigonal cavity.

As a comparison, the binding state of a $[M(phen)_3]^{2+}$ molecule on a silicate surface with no Al substitution was studied. The calculations correspond to the interaction of the metal complex

(21) Allen, M. P.; Tildesley, D. J. *Computer Simulation of Liquids*; Oxford University Press: Oxford, 1987; p 21.
(22) Ando, K.; Kato, S. *J. Chem. Phys.* **1991**, *95*, 5966.
(23) Jayaran, B.; Beveridge, D. L. *J. Phys. Chem.* **1990**, *94*, 4666.
(24) Sato, H.; Yamagishi, A.; Kato, S. *Clay Sci.* **1991**, *8*, 147.

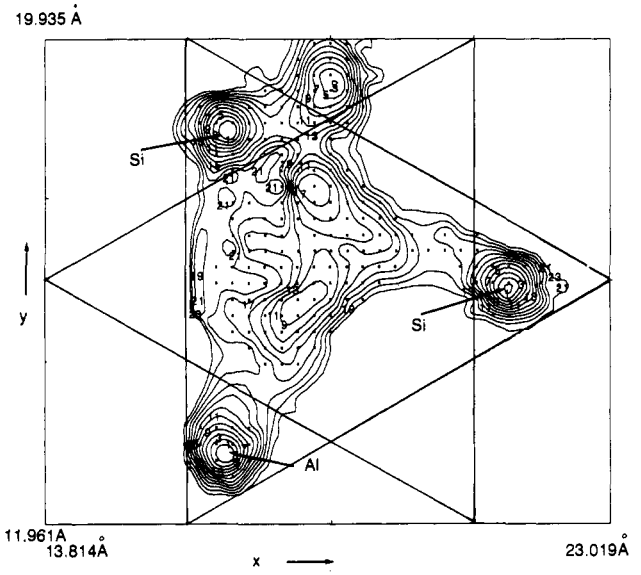

Figure 4. A contour map of the free energy resulting when a $[M(phen)_3]^{2+}$ molecule is bound on a silicate sheet. Each contour spacing is equal to 2 kJ/mol.

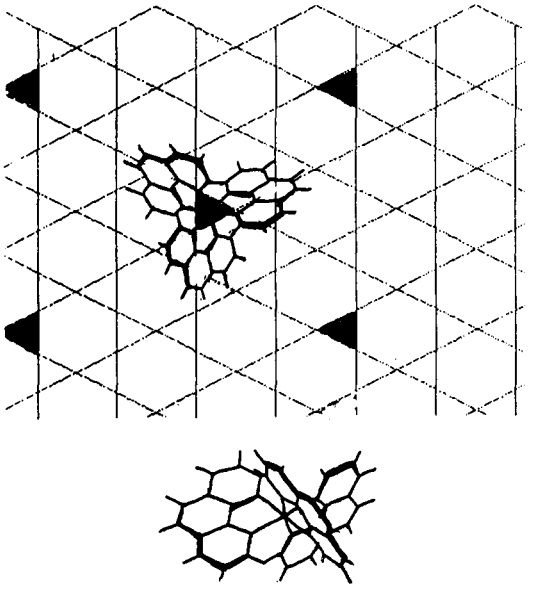

Figure 5. The bound state of Λ $[M(phen)_3]^{2+}$ at the minimum binding energy. The lower and upper pictures are the projections of the bound state onto the y,z and x,y planes, respectively.

with talc or pyrophyllite in water medium. As a result, there exist several shallow potential minima along the x axis, as shown in Figure 6A. The same situations are obtained along the y axis (not shown). Thus the metal complex does not stay at definite positions but moves about on the surface. The C_3 axis of the metal complex orients in the wide region from 60° to 130° with respect to the normal direction (Figure 6B).

(2) Interactions between Two Bound $[M(phen)_3]^{2+}$ Molecules on a Silicate Sheet. To study these interactions, a pair of $[M(phen)_3]^{2+}$ molecules are placed inside the prism as in Figure 2. The upper sheet is then replaced with water medium. This corresponds to the binding of the first two molecules by a negatively charged clay layer in water medium. Such a layer exists when a clay is colloidally dispersed in water. The simulation is started from the configuration in which the central metal ions of two metal complexes are located at the 1 and 2 positions on the lower sheet in Figure 1. This configuration is chosen because our purpose is to analyze the stacking interactions between the bound molecules. For the racemic pair, a Λ isomer is placed at position

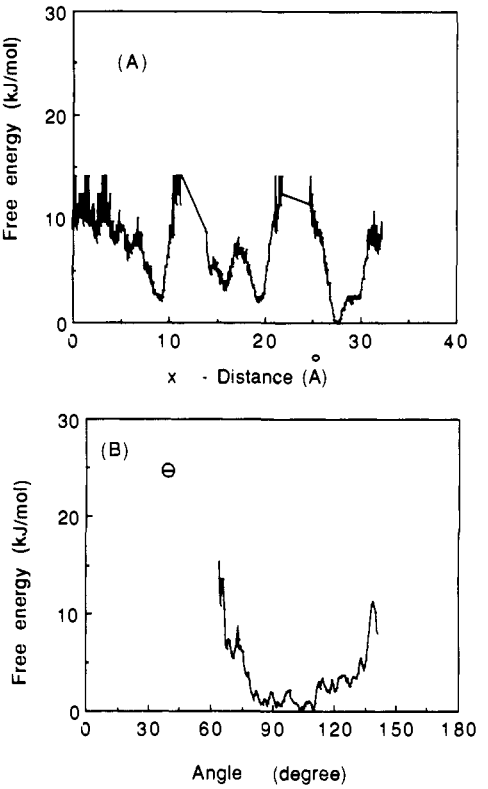

Figure 6. The free energy curves for the binding of Λ $[M(phen)_3]^{2+}$ on a silicate surface with no substitution of Al atoms for Si atoms. The free energy is plotted as a function of (A) the x coordinate and (B) the θ coordinate.

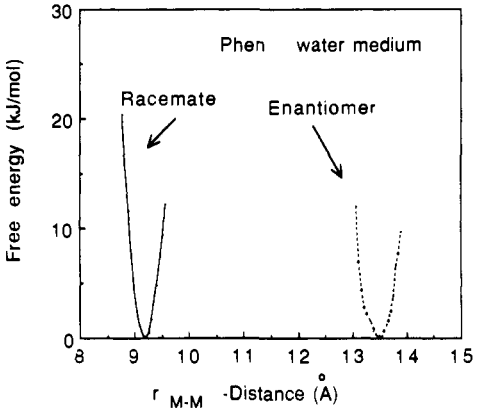

Figure 7. The free energy curves for the binding of the racemic pair (solid curve) and the enantiomeric pair (dotted curve) of $[M(phen)_3]^{2+}$. The free energy is plotted as a function of the intermolecular distance, r_{M-M}.

1 and a Δ isomer at position 2. For the enantiomeric pair, two Λ isomers are placed at positions 1 and 2.

Figure 7 shows the free energy profiles as a function of intermolecular distance (r_{M-M}). The solid and dotted curves indicate the results for the racemic and enantiomeric pairs, respectively. The racemic pair has the minimum free energy at r_{M-M} = 9.2 Å, and the enantiomeric pair, at 13.4 Å. For both the racemic and enantiomeric pairs, the minimum positions are stabilized with free energy barriers higher than 10 kJ/mol. This implies that both pairs form a stable association on a silicate surface. Comparing the free energy profiles between these two cases, the racemic pair forms a more compact association than does the enantiomeric pair.

Figure 8A,B shows the picture resulting when the racemic and enantiomeric pairs of $[M(phen)_3]^{2+}$, respectively, take the lowest binding energy. For the racemic pair, the central metal ion of chelate 1 (Λ isomer) is located above the aluminum atom in the sheet. It orients the C_3 axis perpendicularly with the hydrogen

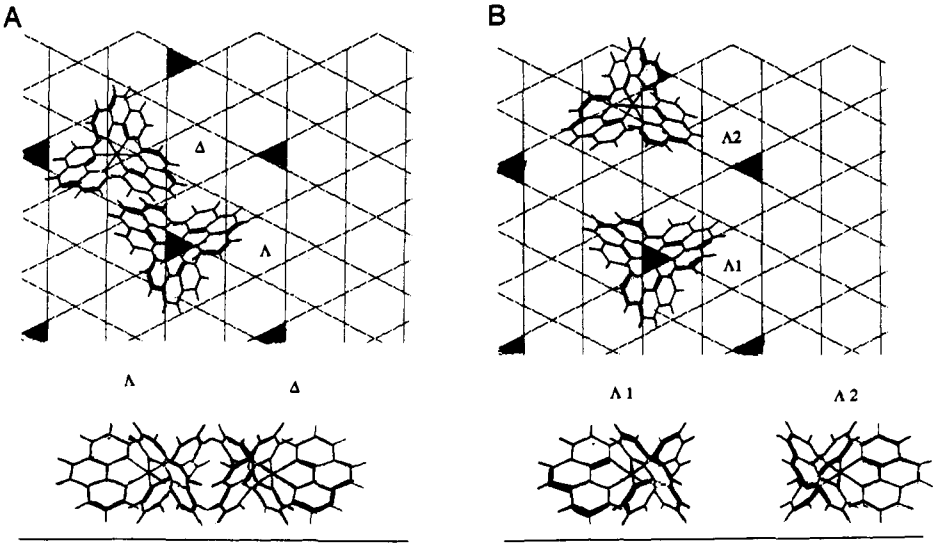

Figure 8. The bound state of a pair of $[M(phen)_3]^{2+}$ molecules at the minimum binding energy. The lower and upper pictures are the projections of the bound state onto the y,z and x,y planes, respectively: (A) a racemic pair and (B) an enantiomeric pair.

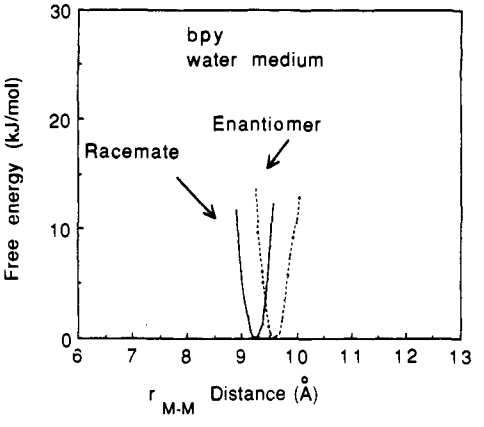

Figure 9. The potential free energy curves for the binding of the racemic pair (solid curve) and the enantiomeric pair (dotted curve) of $[M(bpy)_3]^{2+}$. The free energy is plotted as a function of the intermolecular distance, r_{M-M}.

atom of each ligand located at the center of the ditrigonal cavity in the sheet. The central metal ion of chelate 2 (Δ isomer) is located above a silicon atom in the sheet. It orients in the same way as does chelate 1. One of the ligands in chelate 1 faces closely one of the ligands in chelate 2. The shortest distance between these ligands is less than 4 Å, indicating that van der Waals interactions are dominant among the facing ligands. For the enantiomeric pair, chelate Λ1 is in almost the same binding state as for the racemic pair. Chelate Λ2, however, is located at a position more distant from chelate Λ1. The central metal ion of chelate Λ2 is located above the silicon atom adjacent to the aluminum atom. Since the distances between the ligands of these chelates are longer than 8 Å, there is little contribution of van der Waals interactions in binding the molecules.

Table I gives the mean binding energies for these systems. The mean total binding energy is more negative for the racemic pair than for the enantiomeric pair by 1.5 kJ/mol. The difference mainly lies in the intermolecular term, E_{M-M}, which is less positive for the racemic pair than for the enantiomeric pair by 5.9 kJ/mol.

(3) Interactions between Two Bound $[M(bpy)_3]^{2+}$ Molecules on a Silicate Sheet. Monte Carlo simulations are extended to the case of a pair of bound $[M(bpy)_3]^{2+}$ molecules. The starting positions are the same as in the case of the $[M(phen)_3]^{2+}$ molecules. Figure 9 shows the plots of the free energy of $[M(bpy)_3]^{2+}$ molecules as a function of r_{M-M}. Both racemic and enantiomeric pairs take the minimum free energy at almost the same intermolecular distance, r_{M-M} = 9.3 Å (racemate) and 9.5 Å (enantiomer). Thus it is deduced that these pairs form stable associations with similar compactness.

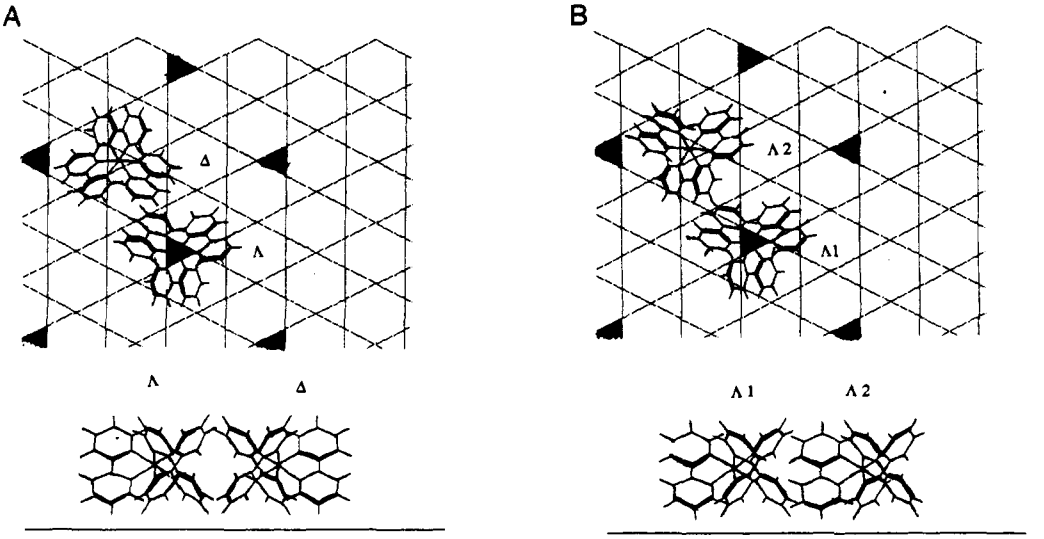

Figure 10. The structure of a bound pair of $[M(bpy)_3]^{2+}$ molecules at the minimum binding energy. The lower and upper pictures are the projections of the bound state onto the y,z and x,y planes, respectively: (A) a racemic pair and (B) an enantiomeric pair.

Table I. Binding Energies

	E^a	$E_{M1-C}{}^a$	$E_{M2-C}{}^a$	$E_{M-M}{}^a$
phen (2+)				
racemate	−704.24	−369.55	−356.84	22.14
enantiomer	−702.72	−368.21	−362.52	28.04
bpy (2+)				
racemate	−648.65	−361.68	−344.56	57.59
enantiomer	−623.32	−352.88	−346.48	76.12
phen (3+)				
racemate	−805.14	−496.06	−473.39	164.33
enantiomer	−931.75	−495.35	−498.14	61.81
en (3+)				
racemate	−1088.99	−551.88	−547.47	10.35
enantiomer	−1093.06	−551.79	−551.52	10.25

[a] All energies are in kJ/mol.

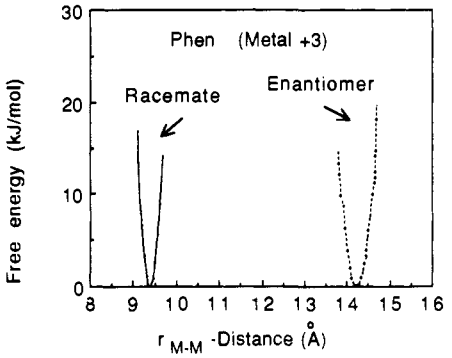

Figure 11. The free energy curves for the binding of the racemic pair (solid curve) and the enantiomeric pair (dotted curve) of $[M(phen)_3]^{3+}$. The free energy is plotted as a function of the intermolecular distance, r_{M-M}.

Figure 10A,B shows the binding states of the racemic and enantiomeric pairs, respectively, at the minimum binding energy. For the racemic pair, both chelates 1 and 2 (Λ and Δ, respectively) orient their C_3 axes perpendicularly to the surface. The hydrogen atoms at the bottoms of both molecules are all located nearly at the centers of the ditrigonal cavities. One of the ligands of chelate 1 faces closely one of the ligands of chelate 2, as already noted for the racemic pair of $[M(phen)_3]^{2+}$. For the enantiomeric pair, chelate Λ1 (Λ isomer) is in almost the same state as for the racemic pair, while chelate Λ2 (Λ isomer) rotates about 60° around the C_3 axis to avoid the steric interference between the facing ligands.

Table I includes the mean binding energies for these pairs. From the table, the racemic pair has a 25.3 kJ/mol lower binding energy than the enantiomeric pair. The difference arises mainly from the intermolecular interaction energy, E_{M-M}, which is less positive for the racemic pair than for the enantiomeric pair by 18.4 kJ/mol.

(4) Interactions between Two Bound $[M(phen)_3]^{3+}$ Molecules on a Silicate Sheet. In order to see the effect on binding of the charges of bound metal complexes, the binding states of a pair of $[M(phen)_3]^{3+}$ molecules were studied. The simulations are carried out in the same way as for a pair of $[M(phen)_3]^{2+}$ molecules. Figure 11 shows the results, in which the free energy is plotted as a function of r_{M-M}. The racemic pair has the minimum free energy at r_{M-M} = 9.4 Å, and the enantiomeric pair, at r_{M-M} = 14.2 Å. Thus the increase of the charge results in more separation of the enantiomeric pair but has little effect on the binding state of the racemic pair.

From Table I, the intermolecular repulsion between the racemic pair is increased more than 7-fold due to the increase of charge from 2+ to 3+. However, the higher binding energy of each metal complex with a silicate surface overcomes the increase of the repulsion.

(5) Interactions between Two Bound $[M(en)_3]^{3+}$ Molecules on a Silicate Sheet. Interactions between two bound $[M(en)_3]^{3+}$ molecules were studied to see the size effect on the stacking interactions. Figure 12 shows the results, in which the free energy is plotted as a function of r_{M-M}. Both the racemic and enantiomeric pairs have the minimum free energy at r_{M-M} = 16.0 Å. At this distance, the bound molecules interact only through electrostatic forces. Thus no stable association is formed for both cases.

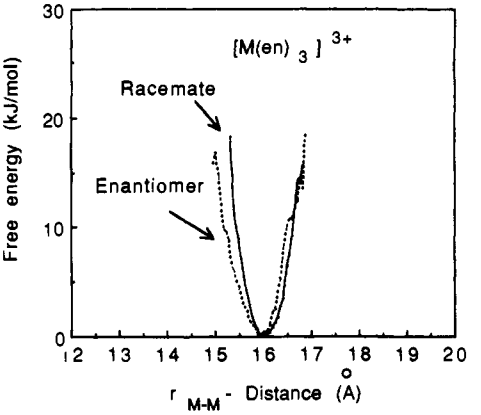

Figure 12. The free energy curves for the binding of the racemic pair (solid curve) and the enantiomeric pair (dotted curve) of $[M(en)_3]^{3+}$. The free energy is plotted as a function of the intermolecular distance, r_{M-M}.

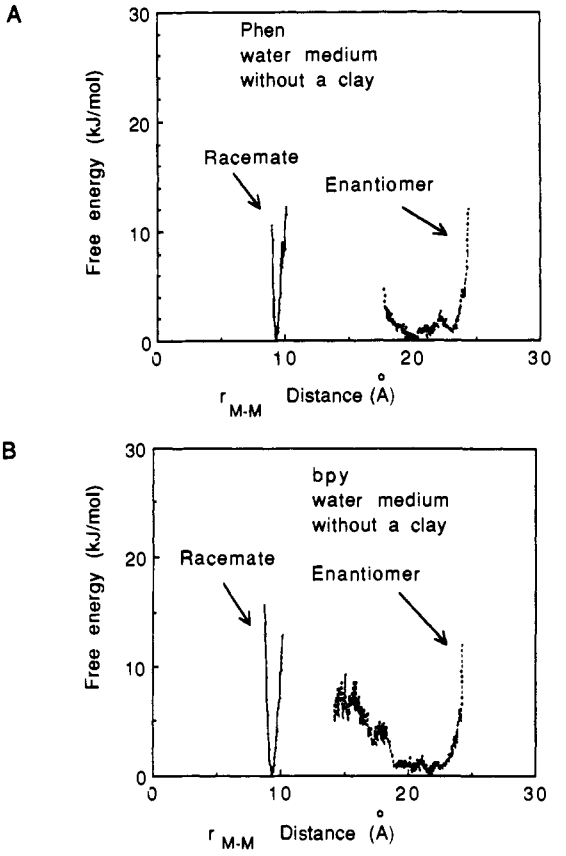

Figure 13. The free energy curves for the racemic pairs (solid curves) and the enantiomeric pairs (dotted curves) of chelates in water medium. The free energy is plotted as a function of the intermolecular distance, r_{M-M}: (A) a $[M(phen)_3]^{2+}$ pair and (B) a $[M(bpy)_3]^{2+}$ pair.

(6) Interactions between the Chelates in Water Medium. In order to clarify the role of the silicate sheet, the interaction between two chelate molecules was studied in the absence of the silicate sheet. The two molecules are placed inside the prism as in Figure 2. The central metal ion of chelate 1 is fixed at the center of the prism. The movement of chelate 2 is limited on the same plane as chelate 1. Figure 13A,B shows the free energy profiles of $[M(phen)_3]^{2+}$ and $[M(bpy)_3]^{2+}$, respectively, as a function of r_{M-M}. The solid and dotted curves represent the results for the racemic and enantiomeric pairs, respectively. For the racemic pair of

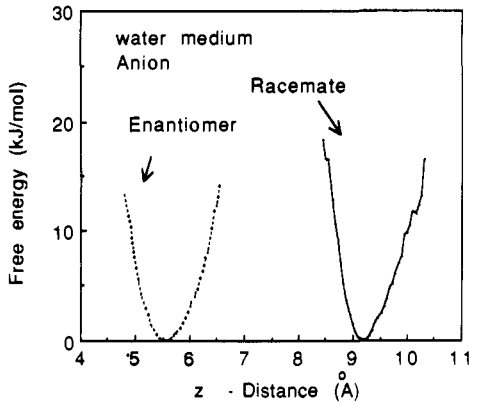

Figure 14. The free energy curves of the binding of the chloride anion for the systems involving the racemic pair (solid curve) and the enantiomeric pair (dotted curve) of $[M(phen)_3]^{2+}$ bound on a silicate sheet. The free energy is plotted as a function of the distance of the anion from the silicate sheet.

Table II. Anion Binding Energies

	E^a	$E_{A\text{-}M1}{}^a$	$E_{A\text{-}M2}{}^a$	$E_{C\text{-}A}{}^a$
phen (water)				
racemate	−269.23	−129.38	−178.57	38.72
enantiomer	−231.47	−128.99	−163.03	60.55

[a] All energies are in kJ/mol.

$[M(phen)_3]^{2+}$, the free energy takes the minimum value at the intermolecular distance $r = 9.4$ Å. This means that the molecules form a stable association even in the absence of a clay. For the enantiomeric pair of $[M(phen)_3]^{2+}$, chelate 2 is separated to the edge of the unit cell, forming no stable association. The same results are obtained for $[M(bpy)_3]^{2+}$ pairs. A stable association is formed at $r_{M\text{-}M} = 9.4$ Å for the racemic pair, while no stable pair is formed for the enantiomeric pair.

(7) Effects of an External Anion on the Binding of $[M(phen)_3]^{2+}$ Molecules. The effect of an anion on the binding of a pair of racemic or enantiomeric $[M(phen)_3]^{2+}$ molecules was studied. A chloride ion is selected as an external anion. As an initial configuration, the racemic and enantiomeric pairs of the metal complexes are placed at the same positions as shown in parts A and B of Figure 8, respectively. Figure 14 shows the results, in which the free energy is plotted as a function of the z coordinate of the chloride ion, $r_{C\text{-}A}$. The ion has the minimum free energy at $r_{C\text{-}A} = 9.2$ and 5.5 Å for the racemic and enantiomeric pairs, respectively. Figure 15A,B shows the positions of the chloride ion at the lowest energy for the systems of the racemic and enantiomeric pairs, respectively. Table II gives the average binding energy of the anion, in which $E_{A\text{-}M1}$, $E_{A\text{-}M2}$, and $E_{C\text{-}A}$ denote the interaction energies with chelate 1, chelate 2, and a silicate surface, respectively. As a result, the chloride ion is stably bound to both the racemic and enantiomeric pairs of $[M(phen)_3]^{2+}$ molecules on a silicate sheet. According to Table II, however, the average binding energy of the anion for the racemic-pair system is about 37.8 kJ/mol lower than for the enantiomeric-pair system. This difference arises from the $E_{C\text{-}A}$ term. That is, the anion in the racemic system undergoes less repulsive energy from the silicate sheet than in the enantiomeric system.

Discussion

The present system is a model of the binding of a $[M(phen)_3]^{2+}$ or $[M(bpy)_3]^{2+}$ molecule by a clay. The binding states are compared between the racemic and enantiomeric pairs of each metal complex. The simulations are started at the configuration that places the two molecules at the closest distance. The following assumptions are made in these calculations: (1) A clay surface is a two-dimensional network of linked $[SiO_4]^{4-}$ and $[AlO_4]^{5-}$ tetrahedra. The contribution of the octahedral sheet is taken into account by adding an OH group at the center of a ditrigonal cavity. (2) Both a silicate sheet and a metal complex have a rigid structure. Thus no structural distortion is induced by the interactions between the sheet and the metal complexes. (3) Water is regarded as a dielectric continuum with a distance-dependent dielectric constant. Thus no molecular interaction of water molecules with the silicate sheet or a metal complex is taken into account.

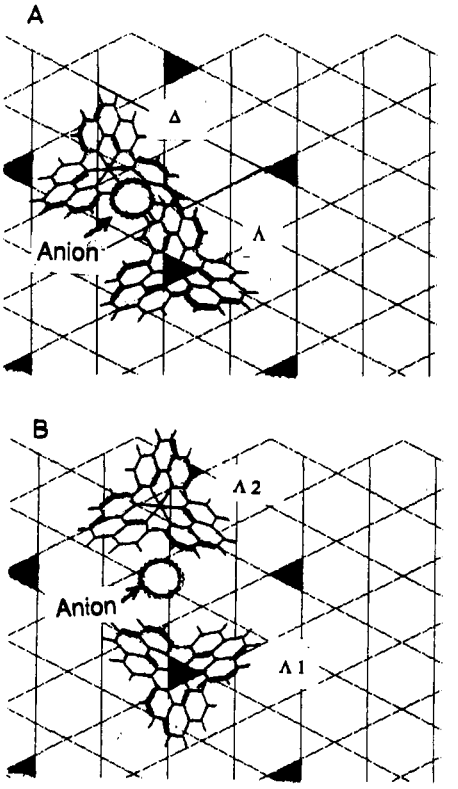

Figure 15. The structure of the chloride anion and a bound pair of $[M(phen)_3]^{2+}$ molecules at the minimum binding energy. The pictures are the projections of the bound state onto the x,y planes: (A) a racemic pair and (B) an enantiomeric pair.

The present model surface (Figure 1) corresponds to the surface of a saponite clay with a CEC of about 1.25 mequiv/g. As for assumption 1, the contribution of an octahedral sheet is important especially when an adsorbed molecule interacts with a clay surface through hydrogen bonding with the OH groups.[25] In the present cases, however, neither $[M(phen)_3]^{2+}$ nor $[M(bpy)_3]^{2+}$ possesses a functional group to form a hydrogen bond. As for assumption 2, the interaction energy between the clay surface and a metal complex is thought to be small enough to induce no structural distortion. One possibility against this assumption is that the pyridyl groups in $[M(bpy)_3]^{2+}$ rotate internally. This may enhance the contribution of van der Waals interactions, leading to the closer stacking of the chelates. No extensive distortion, however, is confirmed in a bound $[M(bpy)_3]^{2+}$ molecule by recent resonance Raman studies.[26] As for assumption 3, water molecules may interact with a silicate surface specifically. Such an interaction is not stereoselective, so that the chirality effects on the intermolecular interactions are expected to be little altered by the presence of water molecules.

In spite of the above simplification, the present Monte Carlo simulations have suggested several important aspects as to the bound states of the metal complexes:

(i) A bound $[M(phen)_3]^{2+}$ molecule is predicted to orient the C_3 axis perpendicularly to the clay surface. This prediction is in accord with previous X-ray and electric dichroism studies, in which both $[M(phen)_3]^{2+}$ and $[M(bpy)_3]^{2+}$ are bound with the C_3 axes at an angle of about 75° with respect to the surface.[9,27] When

(25) Raupach, M.; Slade, P. G.; Janile, L.; Radoslovich, E. W. *Clays Clay Miner.* **1975**, *23*, 181.
(26) Gosh, P. K.; Bard, A. J. *J. Phys. Chem.* **1984**, *88*, 5519.
(27) Taniguchi, M. Ph.D. Dissertation, Tokyo University, 1990; Chapter 4.

the central metal ion takes a position above either an aluminum atom or a silicon atom in a silicate sheet, the hydrogen atom at the bottom of each ligand is located nearly at the center of a ditrigonal cavity (Figure 5). Such geometrical matching between the metal complex and the silicate sheet realizes a definite orientation of the bound metal complex, as previously suspected on a simple molecular model.[4]

(ii) When a $[M(phen)_3]^{2+}$ molecule is adsorbed on a silicate surface with no Al substitution, it does not take a definite binding state (Figure 6A,B). The average binding energy of the metal complex (−148.7 kJ/mol) is much smaller than that for case i (−369.6 kJ/mol). Experimentally this corresponds to the interaction of the metal complex with talc and pyrophyllite. No experimental results have been reported on such systems. As a comparison, the adsorption of $[Ru(bpy)_3]^{2+}$ on porous Vycor glass has been studied by measuring the luminescence from a bound metal complex.[28] According to that study, the metal complex is fixed, with no translational mobility. Probably the metal complex is adsorbed by an ion-exchange mechanism on such a glass surface.

(iii) For $[M(phen)_3]^{2+}$ molecules, a racemic pair forms a more compact association than an enantiomeric pair (Figure 8A,B). In spite of the closer stacking, the repulsive energy is less positive for the racemic pair than for the enantiomeric pair (Table I). It is concluded that van der Waals interactions between the ligands of the associated molecules reduce the electrostatic repulsive energy. Such an effect is absent for the enantiomeric pair because the steric hindrance between the ligands prohibits the metal complexes from having their ligands closely opposed.

(iv) For $[M(bpy)_3]^{2+}$ molecules, both racemic and enantiomeric pairs form associations with nearly equal compactness (Figure 10A,B). In the case of an enantiomeric $[M(bpy)_3]^{2+}$ pair, the steric hindrance between the ligands is avoided by rotating one of the molecules about 60° around the C_3 axis in comparison to the racemic pair. Moreover, the absence of carbon atoms at the 5 and 6 positions in a phenanthroline ligand has an effect in decreasing the repulsive energy.

Recently photophysical studies have been made on the binding state of $[M(bpy)_3]^{2+}$ on a colloidally dispersed clay.[29,30] For example, the intensity of luminescence differs nearly 2-fold between enantiomeric and racemic $[Ru(bpy)_3]^{2+}$ even at the low loading level. Besides, the peak position of the luminescence differs between racemic $[M(bpy)_3]^{2+}$ (605 nm) and enantiomeric $[M(bpy)_3]^{2+}$ (586 nm).[30] The racemate emission falls off rapidly with increased loading from 0 to 50%, whereas the emission from the enantiomeric adsorbates remains almost constant.[30] In explaining these results, a model is presented wherein the racemates are clustered locally, while the enantiomeric ions are more randomly distributed on a clay surface.

Comparing the above model with the present calculations, the calculations suggest that the observed chirality effects are caused by the difference not in compactness but in the relative orientation between the racemic and enantiomeric pairs. The binding energy for the racemic pair is estimated to be 25.3 kJ/mol more negative than that of the enantiomeric pair. This energy difference corresponds to about a 40-nm shift of the wavelength of light at about 600 nm. Therefore it is possible to ascribe the observed shift of the emission peak (19 nm) to the intermolecular interactions between the bound species.

(v) The effect of the charge of a metal complex on the stacking structures is examined by studying $[M(phen)_3]^{3+}$ pairs. The racemic $[M(phen)_3]^{3+}$ pair takes nearly the same structure as the racemic pair of $[M(phen)_3]^{2+}$, while the enantiomeric $[M(phen)_3]^{3+}$ pair has a little greater separation compared to the separation in the enantiomeric $[M(phen)_3]^{2+}$ pair. Thus the increase of the charge of a central metal ion from 2+ to 3+ does not alter the binding structures very much. The validity of these predictions should be examined by studying the adsorptions of trivalent metal complexes such as $[Co(phen)_3]^{3+}$. Racemic $[Co(phen)_3]^{3+}$ and $[Co(bpy)_3]^{3+}$ are reported to be adsorbed in excess over CEC, at least supporting the results of the present calculations.[31]

(vi) Neither a racemic pair nor an enantiomeric pair of $[M(en)_3]^{3+}$ forms a stable association on a silicate surface. In this case, van der Waals interactions between the ligands are too small to overcome the electrostatic repulsions between the positively charged molecules. This is in accord with the experimental results that both racemic and enantiomeric pairs of $[Co(en)_3]^{3+}$ are adsorbed at levels within the CEC.[4b]

(vii) In the absence of a silicate surface, the racemic pairs of $[M(phen)_3]^{2+}$ and $[M(bpy)_3]^{2+}$ are predicted to form stable dimers, while the enantiomeric pairs of these metal complexes dissociate into separated molecules. It is therefore deduced that the role of a silicate surface is most prominent in the case of enantiomeric $[M(bpy)_3]^{2+}$. The enantiomeric pair of $[M(bpy)_3]^{2+}$ forms a stable dimer only in the presence of a silicate surface. On the surface, the repulsive energy between the enantiomers is overcome by the stabilization due to binding with a silicate surface (Table I). The calculated results are compared with the NMR studies on an aqueous solution of $[Ru(phen)_3]^{2+}$.[32] According to those studies, both racemic and enantiomeric $[M(phen)_3]^{2+}$ form dimers at concentrations higher than 0.05 M. One or two anions are included in the associations. In contrast with the calculated results, the enantiomer forms a dimer with a binding constant similar to that of the racemic mixture.

(viii) From Table II, it is predicted that the binding energy of a chloride ion is about 37.8 kJ/mol lower for the bound racemic pair than for the enantiomeric pair. According to X-ray diffraction analyses, racemic $[Ru(phen)_3]^{2+}$ forms a bimolecular layer when it is adsorbed in excess over the CEC. A counter anion is included between the upper and lower adsorbate layers.[8b,9] Contrary to this, the enantiomer forms a monolayer when it is adsorbed at levels within the CEC. No anion is included in the adsorbate. These results imply that the binding stability of an anion is an important factor in determining whether the chelates are adsorbed at levels within or beyond the CEC. Although the present calculations correspond to the adsorption of the chelate at low loading, the results in Table II are considered to be consistent with these experimental observations. For the racemic mixture, an anion is so strongly bound to a clay–chelate adduct that it may continue to stay at high loading. As a result, the adsorption of the racemic chelate goes beyond the CEC, including external anions. For the enantiomeric system, an anion is so weakly bound to a clay–chelate adduct that it is dissociated at high loading. Thus the adsorption may stop at the CEC amount. For the racemic pair, the anion is located above the bound molecules as shown in Figure 15A. At this position, it experiences smaller repulsive interaction from a negatively charged silicate sheet. This situation is realized because the racemic pair forms such a compact dimer that there remains no empty space between the chelates. In conclusion, the closer stacking of the racemic pair of $[M(phen)_3]^{2+}$ results in more efficient shielding of the negative charge of a silicate sheet. As a result, the chelates are adsorbed in excess over the CEC, forming a bimolecular layer with an external anion.

Acknowledgment. The calculations were performed at the IMS Computer Center, Okazaki, Japan.

(28) Shi, W.; Wolfgang, S.; Strekas, T. C.; Gafney, H. D. *J. Phys. Chem.* **1985**, *89*, 974.
(29) Joshi, V.; Gosh, P. K. *J. Am. Chem. Soc.* **1989**, *111*, 5604.
(30) Kamat, P. V.; Gopidas, K. R.; Mukherjee, T.; Joshi, V.; Kotkar, D.; Pathak, V. S.; Ghosh, P. K. *J. Phys. Chem.* **1991**, *95*, 10009.
(31) Swartzen, A.; Matijevic, E. *J. Colloid Interface Sci.* **1975**, *50*, 144.
(32) Masuda, Y.; Yamatera, H. *Bull. Chem. Soc. Jpn.* **1984**, *57*, 58.